The EMBO Journal (2007) 26, 2262–2273 | © 2007 European Molecular Biology Organization | All Rights Reserved 0261-4189/07
www.embojournal.org

THE EMBO JOURNAL

Proteomic screen defines the Polo-box domain interactome and identifies Rock2 as a Plk1 substrate

Drew M Lowery[1,4], Karl R Clauser[2,4], Majbrit Hjerrild[1,3,4], Dan Lim[1], Jes Alexander[1], Kazuhiro Kishi[1], Shao-En Ong[2], Steen Gammeltoft[3], Steven A Carr[2,*] and Michael B Yaffe[1,2,*]

[1]Departments of Biology and Biological Engineering, Center for Cancer Research, Massachusetts Institute of Technology, Cambridge, MA, USA, [2]Broad Institute of MIT and Harvard, Cambridge, MA, USA and [3]Department of Clinical Biochemistry, Glostrup Hospital, Glostrup, Denmark

Polo-like kinase-1 (Plk1) phosphorylates a number of mitotic substrates, but the diversity of Plk1-dependent processes suggests the existence of additional targets. Plk1 contains a specialized phosphoserine–threonine binding domain, the Polo-box domain (PBD), postulated to target the kinase to its substrates. Using the specialized PBD of Plk1 as an affinity capture agent, we performed a screen to define the mitotic Plk1-PBD interactome by mass spectrometry. We identified 622 proteins that showed phosphorylation-dependent mitosis-specific interactions, including proteins involved in well-established Plk1-regulated processes, and in processes not previously linked to Plk1 such as translational control, RNA processing, and vesicle transport. Many proteins identified in our screen play important roles in cytokinesis, where, in mammalian cells, the detailed mechanistic role of Plk1 remains poorly defined. We go on to characterize the mitosis-specific interaction of the Plk1-PBD with the cytokinesis effector kinase Rho-associated coiled–coil domain-containing protein kinase 2 (Rock2), demonstrate that Rock2 is a Plk1 substrate, and show that Rock2 colocalizes with Plk1 during cytokinesis. Finally, we show that Plk1 and RhoA function together to maximally enhance Rock2 kinase activity *in vitro* and within cells, and implicate Plk1 as a central regulator of multiple pathways that synergistically converge to regulate actomyosin ring contraction during cleavage furrow ingression.

The EMBO Journal (2007) **26,** 2262–2273. doi:10.1038/sj.emboj.7601683; Published online 19 April 2007
Subject Categories: signal transduction
Keywords: phosphopeptide-binding domain; Polo-box domain; Polo-like kinase; proteomics; signal transduction

*Corresponding authors. SA Carr, Broad Institute of MIT and Harvard, 7 Cambridge Center, Cambridge MA 02142, USA.
E-mail: scarr@broad.mit.edu or MB Yaffe, Departments of Biology and Biological Engineering, Center for Cancer Research, Massachusetts Institute of Technology, Building E18-580, 77 Massachusetts Avenue, Cambridge, MA 02139, USA. Tel.: +1 617 452 2103; Fax: +1 617 452 4978; E-mail: myaffe@mit.edu
[4]These authors contributed equally to this work

Received: 27 August 2006; accepted: 14 March 2007; published online: 19 April 2007

Introduction

In eukaryotic cells, Polo-like kinase-1 (Plk1) and related orthologues perform a wide variety of essential functions during mitosis (Barr *et al*, 2004; Glover, 2005; van de Weerdt and Medema, 2006). Levels of Plk1 peak in late G2 and early M, accompanied by dramatic changes in subcellular localization as cells transit through various mitotic stages (Golsteyn *et al*, 1994). During interphase and early prophase, Plk1 resides primarily at the centrosome, where it facilitates centrosome maturation, separation, and microtubule nucleation during late prophase and prometaphase (Lane and Nigg, 1996; Rapley *et al*, 2005; De Luca *et al*, 2006). By metaphase, a fraction of Plk1 has relocalized to the kinetochores, where it seems to be involved in regulating aspects of spindle checkpoint function and the metaphase–anaphase transition (Ahonen *et al*, 2005; Goto *et al*, 2006). During anaphase, Plk1 is concentrated in the spindle midzone, where it probably facilitates microtubule sliding, while following chromosome segregation, Plk1 remains in the central spindle and midbody, where it participates in ingression of the cleavage furrow (Neef *et al*, 2003; Liu *et al*, 2004). Particularly prominent cytokinetic phenotypes are observed in budding and fission yeast, where mutations in the respective Plk1 orthologues, Cdc5 and Plo1, result in incomplete assembly of actomyosin and septin ring structures along with delayed and improper deposition of septal material (Lee *et al*, 2005; Yoshida *et al*, 2006).

Although these and related mutational studies have provided many insights into Cdc5/Plo1 function in simple model organisms, the diversity of Plk1 functions in higher eukaryotes makes it difficult to comprehensively identify Plk1-regulated pathways or define the bulk of the Plk1 interactome using standard molecular genetics techniques. Separation of function alleles are hard to identify owing to the presence of a single common binding pocket and substrate phosphorylation cleft shared by most, if not all substrates (Cheng *et al*, 2003; Elia *et al*, 2003b). Full genetic disruption of the *Drosophila* Plk1 orthologue, polo, causes embryonic lethality (Donaldson *et al*, 2001), whereas full depletion of the *Xenopus* Plk1 orthologue, Plx1, prevents mitotic entry (Qian *et al*, 2001).

More recently, RNA interference has been used to examine the effect of Plk1 depletion in human cell lines, revealing a marked dependence of phenotype on the particular genetic background of the cell. In tumor-derived cell lines, depletion of Plk1 causes apoptosis along with mitotic catastrophe, making the delineation of specific Plk1 functions difficult (Spankuch-Schmitt *et al*, 2002; Liu *et al*, 2006). In other immortalized cell lines, depletion of Plk1 causes a delay in mitotic entry with subsequent arrest at prometaphase, preventing analysis of later phenotypes without sensitization strategies to avoid activation of various mitotic checkpoints. If both the DNA damage and spindle checkpoints are

bypassed, Plk1-depleted cells can complete an apparently normal mitosis; however, chromosome segregation fails (van Vugt *et al*, 2004a, b). In non-transformed cell lines, depletion of Plk1 causes only very minor cell-cycle defects, although co-depletion of p53 mimics the cell death phenotypes seen in tumor-derived cell lines (Liu *et al*, 2006). The various Plk1-depletion phenotypes are complicated by varying degrees of Plk1 knockdown, as a 90% knockdown of Plk1 in HeLa cells can allow normal mitotic processes whereas an ~100% depletion completely blocks cell-cycle progression (Liu *et al*, 2005, 2006).

In an effort to more comprehensively elucidate the substrates and interacting proteins of Plk1, we pursued a biochemical/proteomic approach. All Plks have a similar protein architecture including an N-terminal Ser/Thr kinase domain and a conserved C-terminal Polo-box domain (PBD) (Figure 1A). The PBD of Plks was previously identified in our lab as a pSer/pThr-binding module that specifically recognizes Ser-[pSer/pThr]-Pro/X motifs on peptides with low micromolar affinity (Elia *et al*, 2003a). Phospho-dependent ligand recognition by the PBD is necessary for the targeting of Plk1 to specific substrates (i.e. processive phosphorylation), as well as for the dynamic re-localization of Plk1 to specific subcellular structures during mitosis where other Plk1 targets reside (i.e. distributive phosphorylation) (Lowery *et al*, 2005). We therefore performed affinity purification and mass spectrometry studies to identify Plk1 PBD-interacting proteins from U2OS cells at different stages of the cell cycle.

Our strategy was to define all putative interacting partners, and then select one particular sub-network to investigate in more detail at the molecular level. We identified approximately 600 proteins that are members of phosphorylation-dependent Plk1 PBD interacting complexes. These proteins are known to be involved in a wide variety of mitotic processes, including processes not previously thought to be regulated by Plk1. We chose to focus on the roles of Plk1 in regulating cytokinesis. The requirement for Plk1 and its orthologues for proper initiation and completion of cytokinesis has been well established in unicellular organisms (Ohkura *et al*, 1995; Song and Lee, 2001) and *Drosophila* (Carmena *et al*, 1998), and several previously described PBD-associated proteins are known to play roles in this process in mammalian cells (Neef *et al*, 2003; Zhou *et al*, 2003; Liu *et al*, 2004), although exactly how Plk1 fits into the complete cytokinesis network is unclear. One of the major upstream regulators of cytokinesis is RhoA, which, together with its downstream targets, controls the formation and constriction of the actomyosin ring at the cleavage furrow (Glotzer, 2005). The functions of Plk1 and Rho GTPases may be linked, as cytokinesis-specific GEFs for Rho were recently identified as Plk targets both in mammalian cells (Niiya *et al*, 2006) and by our recent work in budding yeast (Yoshida *et al*, 2006).

We now report that Plk1 functions in multiple parallel overlapping pathways with RhoA, and directly interacts with a subset of critical effectors of RhoA. We demonstrate that Plk1 and RhoA synergize to maximally activate the cytokinetic protein kinase Rock2 *in vitro* and within cells, and that Plk1 and Rock2 interact directly *in vivo* in a phosphorylation-dependent mitosis-specific manner, with maximal colocalization at the midbody during cytokinesis.

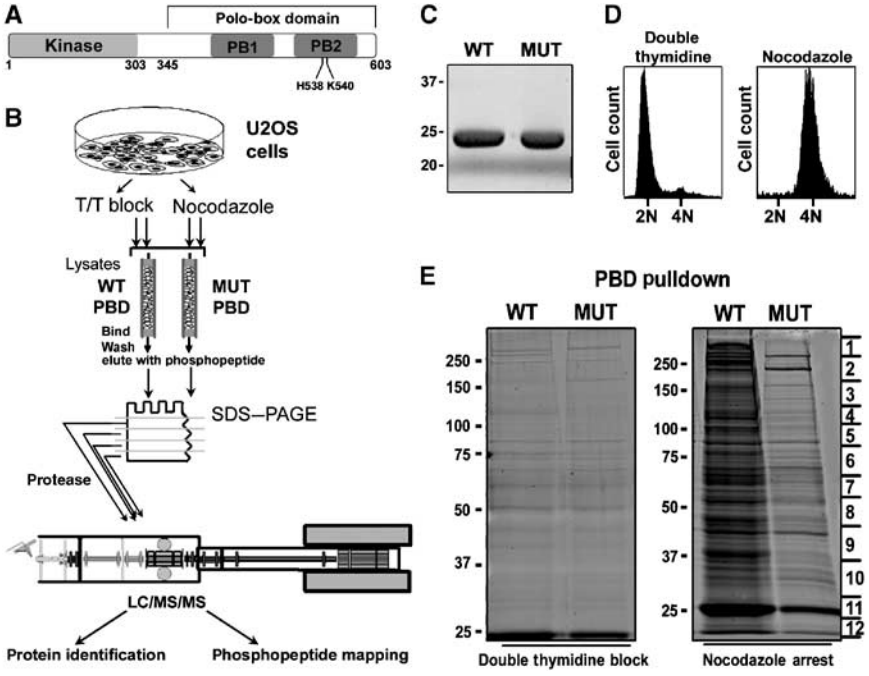

Figure 1 The PBD of Plk1 preferentially binds ligands in mitosis. (**A**) Domain structure of Plk1. Residues His-538 and Lys-540 are required for phosphopeptide binding by the PBD. (**B**) Experimental strategy for identifying cell-cycle-dependent PBD ligands. (**C**) Purity and equivalence of recombinant wild-type (WT) and mutant (MUT) PBDs used for interaction screening. Samples were analyzed by SDS–PAGE and stained with Coomassie blue. (**D**) U2OS cells were synchronized at the G1/S transition by a double thymidine block or in M-phase by nocodazole treatment, and DNA content analyzed by flow cytometry. (**E**) WT and MUT PBD were used to pull down interaction partners from double thymidine blocked or the nocodazole-arrested U2OS cell lysates. Bound proteins were separated by SDS–PAGE and visualized by SYPRO Ruby staining. Lines on the right of gel indicate where gel was cut before subsequent mass spectrometry analysis with each labeled section correlated with Supplementary Table S1.

Results and discussion

The Plk1 PBD shows mitosis-specific interactions with many proteins involved in diverse aspects of cell division

To identify potential targets of Plk1, we examined the ability of the isolated PBD to bind to proteins in a cell cycle-dependent manner. Recombinant Plk1 PBD was expressed in bacteria and purified to homogeneity (Figure 1C). We also purified a His-538 Ala/Lys-540 Met double mutant form of the PBD, which does not bind to phosphorylated ligands (Elia *et al*, 2003b) and therefore serves as an optimal negative control to reveal sticky nonspecific interactions or phospho-independent protein–PBD interactions that might arise from high abundance. The wild-type and mutant PBD proteins were crosslinked to Sepharose CN-4B beads and used as an affinity matrix. Human osteosarcoma U2OS cells were arrested at the G1/S transition by a double thymidine block or arrested in mitosis by treatment with nocodazole. Cell-cycle synchronization was verified by FACS (Figure 1D). Lysates from these two cell populations were prepared and equal amounts of total protein were applied to columns containing either the wild-type or mutant PBD column. After extensive washing with a near neutral-pH medium-salt buffer that is not expected to disrupt complexes, PBD-interacting proteins were eluted off the columns by competition with an optimal PBD-binding phospho-peptide (YMQS-pT-PK) (Elia *et al*, 2003a). The recovered proteins were then separated by SDS–PAGE and visualized by SYPRO Ruby staining (Figure 1B, top).

Both the wild-type and mutant PBD bound very weakly, and with similar affinity, to a variety of proteins in the G1/S cell lysate. In marked contrast, the wild-type PBD, but not the mutant PBD, showed very strong binding to a large number of proteins in the mitotic cell lysates (Figure 1E). The darkest band at 25 kDa is the PBD itself, indicating that there is some leeching of the PBD from the column. These observations suggest that the Plk1 PBD can specifically interact with many mitotic proteins in a phospho-dependent manner. Furthermore, because Plk1 has been reported to interact with microtubules (Feng *et al*, 1999), we used nocodazole treatment to obtain mitotically arrested cells, as this drug depolymerizes microtubules and should therefore minimize potential indirect interactions of the PBD with other microtubule-interacting proteins. The affinity-based purification assay shown in Figure 1E could either isolate mitotic proteins that bound directly to the PBD, or proteins that were not themselves direct PBD interactors but instead were components of larger PBD-associated complexes. The specificity of PBD binding was therefore investigated by Far-Western blotting. Many of the mitotic proteins captured with the wild-type PBD were capable of direct interaction. In contrast, none of the proteins that were retained by the mutant PBD showed a strong detectable interaction with the wild-type PBD in this assay (Figure 2A).

To examine the extent to which the binding of mitotic ligands to the PBD is dependent upon phosphorylation, nocodazole-arrested cell lysates were dephosphorylated with λ-phosphatase before the PBD pull-down. As shown in Figure 2B, both the number of recovered ligands and intensity of ligand binding were greatly reduced after phosphatase treatment of the mitotic cell lysates. Next, to investigate if any of the Plk1 PBD-interacting proteins were also potential Plk1 substrates, the affinity-purified proteins were incubated with a constitutively active mutant of full-length Plk1, Plk1-T210D, in the presence of [γ-^{32}P]ATP. As shown in Figure 2C, incubation with Plk1-T210D resulted in the direct phosphorylation of many of these PBD-interacting proteins. Taken together, the data in Figures 1 and 2 strongly support a model where the PBD facilitates the interaction of Plk1 with a wide range of mitotic targets that have undergone prior priming phosphorylation during mitosis, and indicates that a subset of the interacting proteins are themselves Plk1 substrates.

Liquid chromatography tandem mass spectrometry (LC/MS/MS) was used to identify the mitotic PBD-interacting proteins. Each lane of the gel from the nocodazole-arrested

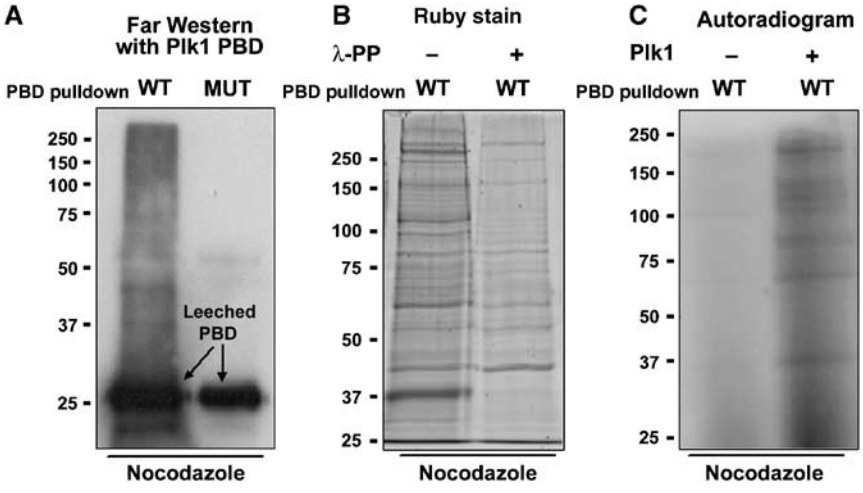

Figure 2 Mitotic proteins bind to the PBD in a phospho-dependent manner and are substrates of Plk1. (**A**) Direct binding of PBD-interacting proteins. Proteins interacting with the wild-type (WT) and mutant (MUT) PBD from nocodazole-arrested U2OS cell lysates (Figure 1B) were transferred to PVDF membrane and analyzed for direct binding by Far-Western analysis using the WT PBD as a probe. (**B**) Phosphorylation-dependent PBD interactions. Nocodazole-arrested U2OS cell lysates were incubated with (+) or without (−) λ-protein phosphatase before WT-PBD pull-down. The bound proteins were separated by SDS–PAGE and visualized by SYPRO Ruby staining. (**C**) Plk1 phosphorylation of PBD-interacting proteins. Wild-type PBD was used to pull down interacting proteins from nocodazole-arrested U2OS cell lysates. The proteins were incubated with or without active Plk1 and [γ-^{32}P]ATP, separated by SDS–PAGE, and visualized by autoradiography.

cell lysates in Figure 1E was excised, cut into 12 pieces as indicated (Figure 1E), and subjected to in-gel digestion with trypsin. The extracted peptide mixtures were then separated using reverse phase HPLC, which was coupled to an LTQ-FT hybrid ion trap Fourier transform mass spectrometer for peptide identification (Figure 1B, bottom), and the corresponding proteins identified by database searching. For each protein, the relative ratio of wild-type/mutant PBD-bound abundances was determined using the sum of the extracted ion current measured for each sequenced peptide precursor ion in the intervening MS scans of the LC/MS/MS chromatogram. Proteins were then categorized as being wild-type specific (peptide ions present only in the wild-type PBD eluents), wild-type enriched (peptide ions present at $>$20-fold intensity in the wild-type PBD eluents compared to the mutant PBD eluents), and nonspecific (peptide ions present at $\leqslant$20-fold intensity in the wild-type versus mutant PBD eluents). In total, we identified 622 distinct proteins that were at least 20-fold more abundant in the wild-type PBD pull-down compared to the mutant H538A/K540 M PBD pull-down and were considered to be potential PBD interaction partners (Supplementary Table S1). All proteins were characterized according to GO categories defining their molecular function (GO Consortium, 2001) (Figure 3A).

We selected a small random subset of proteins identified in the mass spectrometry-based screen for further validation based on the availability of antibodies: Lamin A, Cofilin, MCMs, the protein kinase CK2 alpha, myosin phosphatase targeting subunit 1 (MYPT), and Rock2. Pull-downs from mitotic lysates followed by immunoblotting confirmed that all these proteins preferentially interacted with wild-type PBD compared to the mutant PBD (Supplementary Figure S1A). The cell-cycle-dependent interaction of the selected proteins with the PBD was investigated by performing *in vitro* pull-down assays with lysates from double thymidine blocked (G1) and nocodazole-treated (M) cells. As shown in Supplementary Figure S1B, interactions between the PBD and all of these proteins were mitotic specific. To investigate the requirement for phosphorylation, mitotic lysates were treated with λ-protein phosphatase before PBD pull-downs and immunoblotting. In each case, interaction of these proteins with the PBD was either eliminated or substantially reduced following phosphatase treatment (Supplementary Figure S1C). Thus, all six of the interactions tested were mitotic phosphorylation-dependent interactions.

The complete set of proteins identified in our PBD interactome included proteins previously demonstrated to associate with Plk1 such as MCMs (Tsvetkov and Stern, 2005), septins (Song and Lee, 2001), anillin (shown to be a Plkl substrate *in vitro*; Straight *et al*, 2005), and members of the 20S proteasome complex (Feng *et al*, 2001). Some other known endogenous Plk1-interacting proteins, such as Cdc25C, were not identified in this screen, likely as a result of our nocodazole treatment/spindle checkpoint arrest strategy, which appeared to enrich for late mitotic targets. Plk1 targets such as Cdc25C and Wee1 are thought to play a role in entry into mitosis, and thus might not bind to Plk1 once mitosis is underway. Additional Plk1 interactors, such as Bub3, are only expected to be engaged after the spindle checkpoint is extinguished.

Most of the PBD-interacting proteins identified in this study have not been previously reported. Many of those proteins participate in a broad range of cellular functions that show distinct changes during mitosis, transcription, translation, splicing, and metabolism (Figure 3A). Intriguingly, although protein synthesis is necessary for mitotic entry and progression, the overall rate of protein synthesis in mitotic cells has been reported to be markedly decreased to 25–30% of the rate seen in interphase cells (Tarnowka and Baglioni, 1979). At the same time, the synthesis of a number of proteins including c-myc is enhanced during mitosis (Kim *et al*, 2003). Transcription and mRNA splicing has also been shown to be inhibited during mitosis (Shin and Manley, 2002). The metabolic state of mitotic cells also undergoes significant alterations in order to accommodate disruption and distribution of membrane compartments and components (Warren, 1993). Recently, a transcriptional coactivator protein, Ndd1, has been discovered to be a direct substrate of Cdc5, the yeast Plk1 orthologue. Cdc5 was recruited to specific promoters where it phosphorylated Ndd1 to activate transcription of cell-cycle-regulated genes involved in mitotic progression (Darieva *et al*, 2006). Plk1 has also been shown to regulate the nuclear translocation of the transcription factor HSF1 (Kim *et al*, 2005). Thus, we anticipate further elucidation of the role of Plk1 in these processes.

Bioinformatic analysis reveals that Plk1 PBD ligands are enriched in Ser-[Ser/Thr]-Pro motifs and are potential Plk1 substrates

In order to help distinguish between indirect and direct interactors, each of the PBD-interacting proteins identified by mass spectrometry was evaluated for the presence of an optimal PBD recognition motif. Isolated phosphopeptides bind to the Plk1 PBD through the optimal consensus motif S-[pS/pT]-[P/X], where the Ser residue preceding the pSer/pThr makes three hydrogen-bonding interactions with the PBD (one through a bound water molecule) and contributes significantly to ligand affinity (Elia *et al*, 2003b). As seen in Figure 3B, PBD recognition motifs were identified in 47.3% of the wild-type-specific PBD-interacting proteins and 41.3% of the wild-type-enriched interactions. In contrast, only 16.2% of the nonspecific PBD-interacting proteins contained this motif. To determine whether these values were statistically significant, we generated 2000 'mock' protein data sets by randomly selecting either 622 (the total number of combined wild-type PBD-specific or -enriched interactions; Figure 3B, column 1, red boxes) or 277 proteins (the total number of nonspecific interactions; Figure 3B, column 1, gray box) from the current human NCBI RefSeq collection, and examined these data sets of randomly selected proteins for the percentage of proteins containing S-[S/T]-P motifs. As shown in Supplementary Figure S2A and B, the distribution of the number of protein in each of the random data sets containing S-[S/T]-P motifs was roughly normally distributed, with the same average value of 31.4%. The percentage of PBD-specific or -enriched interacting proteins containing S-[S/T]-P motifs that we identified in our mass spectrometry-based screen (average value 45.3%) was over 7 s.d. above the mean from that expected for a similar sized collection of random proteins (Supplementary Figure S2B). Likewise, the percentage of PBD nonspecific interacting proteins containing S-[S/T]-P motifs was over 5 s.d. below that expected (Supplementary Figure S2A). Thus, our non-biased method for identifying PBD interactors greatly enriched for proteins that contained the optimal motifs necessary for PBD binding, suggesting that the

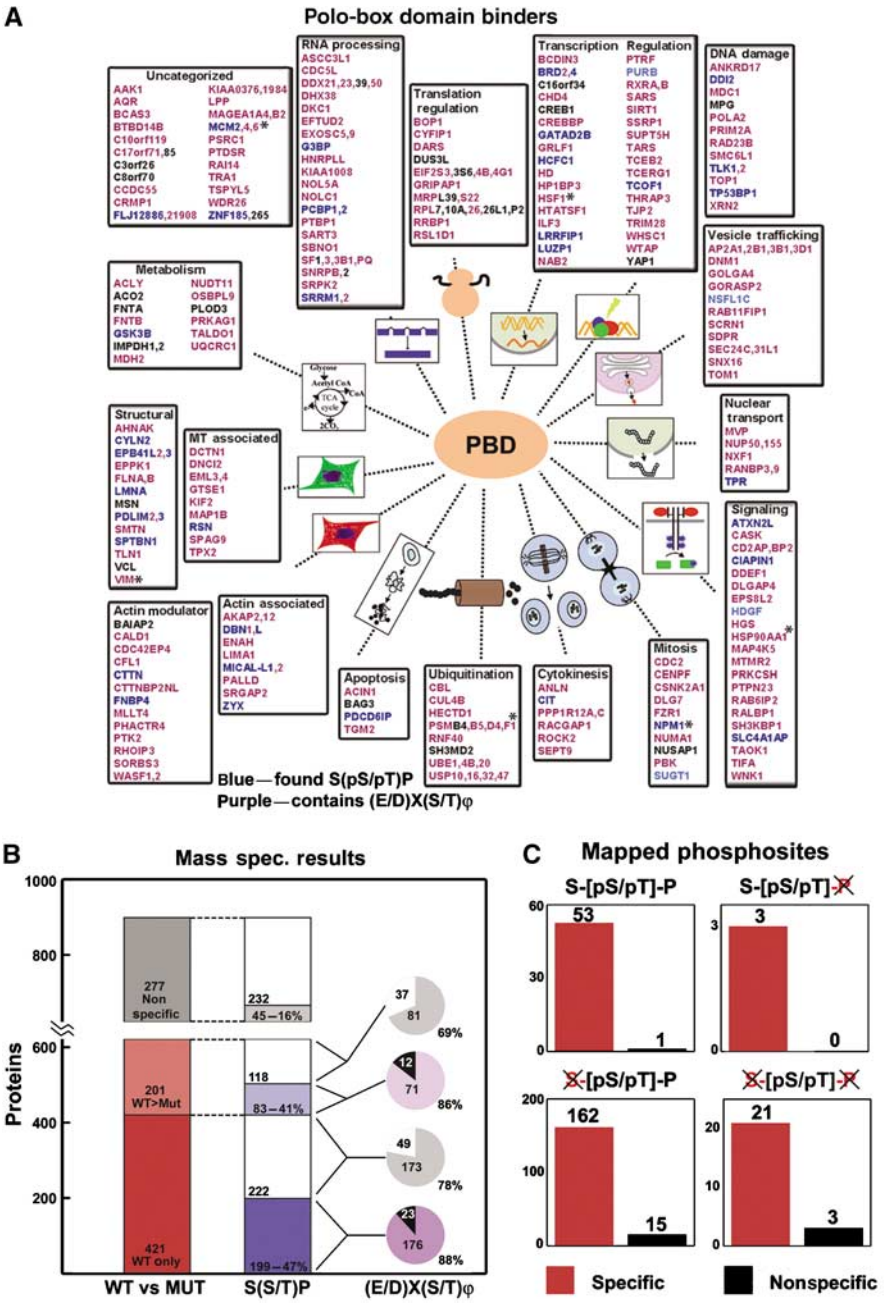

Figure 3 The PBD interactome. (**A**) Only wild-type (WT) PBD-specific or -enriched interacting proteins that contain at least one match to the optimal PBD-binding motif (S-[S/T]-P) are shown ((B), blue boxes, column 2). Proteins were categorized according to their known biological function by GO terms. Blue text indicates those proteins in which we were able to map at least one S-[*pS/pT*]-P site; dark blue indicates those that also contain an optimal Plkl phosphorylation site, whereas light blue indicates those that do not. For the remaining proteins, those shown in purple contain an optimal Plk1 (E/D)X(S/T) φ phosphorylation site, whereas those shown in black do not. Previously known Plk1 interactors are indicated with an asterisk. (**B**) Summary statistics of proteins identified by mass spectrometry from Plk1 PBD pull-down assays in nocodazole-arrested U2OS cells. Proteins were divided into three categories based on specificity for the WT versus mutant (MUT) PBD. Dark red denotes proteins that bound only to the WT PBD; light red, proteins with ⩾20-fold enhanced binding to WT PBD; dark gray, proteins with <20-fold enhanced binding to WT PBD. The presence of optimal PBD-binding S-[S/T]-P motifs is shown by dark and light blue and gray filled bars in the second column. White boxes in the second column correspond to identified interacting proteins that do not contain the optimal PBD-binding motif. Potential Plk1 (E/D)X(S/T)φ phosphorylation sites are indicated by purple and gray wedges in pie charts. (**C**) A subset of phosphorylation sites in the WT specific/enriched versus nonspecific PBD-interacting proteins were mapped by mass spectrometry. Mapped sites were categorized into those that matched the optimal PBD-binding motif (S-[*pS/pT*]-P), the minimal peptide PBD-binding motif (S-[*pS/pT*]), the minimal cyclin-dependent kinase phosphorylation motif ([*pS/pT*]-P), or none of the above ([*pS/pT*]).

optimal PBD-binding motif for isolated phosphopeptides likely functions in an analogous way for many full-length phosphoprotein ligands.

The wild-type PBD-specific or -enriched interacting proteins were also evaluated for the presence of potential Plk1 phosphorylation sites [E/D]-X-[S/T]-[F/L/I/Y/W/V/M] (Nakajima *et al*, 2003). Among the 282 proteins that contain a PBD recognition motif, this motif was found in 88% of the proteins. In contrast, among the 340 proteins that do not contain a PBD recognition motif, this phosphorylation motif

was present in 75% of the proteins (Figure 3B). We performed a similar statistical analysis for putative Plk1 phosphorylation sites in random protein data sets containing either 282 proteins (the number of wild-type PBD-specific or -enriched interactions containing S-[S/T]-P motifs; Figure 3B, blue boxes, column 2) or 340 proteins (the number of wild-type PBD-specific or -enriched interactions not containing S-[S/T]-P motifs; Figure 3B, white boxes, column 2). This revealed a similar mean value of 74.4% (Supplementary Figure S2C and D). The co-occurrence of a Plk1 phosphorylation motif in the S-[S/T]-P motif-containing PBD-specific or -enriched proteins found in our mass spectrometry-based screen was nearly 5 s.d. greater than that expected by chance alone in a randomly selected set of proteins (Supplementary Figure S2D). In contrast, for the PBD-specific or -enriched proteins found in our mass spectrometry-based screen that lacked S-[S/T]-P motifs, the occurrence of a Plk1 phosphorylation motif was the same as that expected by random chance (Supplementary Figure S2C). We interpret these findings as evidence that Plk1 interactors capable of binding directly to the PBD are also likely to be Plk1 substrates, whereas proteins in complexes with direct PBD interactors may be less likely to be Plk1 substrates than the PBD interactors themselves.

The mass spectrometry analysis of the PBD-interacting proteins also resulted in the mapping of 247 phosphophorylation sites (Figure 3C and Supplementary Table S2), although this was not the primary intent of our study. The majority of mapped phosphorylation sites were derived from the gel band tryptic digests of our PBD pull-downs with a few from a TiO2 IMAC using a tryptic digest of an aliquot of the PBD pull-downs. Within the tryptic peptides, many of the phosphorylation motifs are present in a sequence context that is not readily amenable to binding and elution from a reversed-phase column and ionization/fragmentation by MS/MS (i.e. too short, long, hydrophobic, hydrophilic, or contain too many nearby basic residues). Therefore, we expect to observe only a portion of phosphopeptides actually present. In 282 proteins that were identified as wild-type PBD-specific or -enriched interacting proteins (Figure 3B, column 2, blue boxes), we were able to map 49 phosphorylation sites in 43 proteins that exactly matched the Ser-(pSer/pThr)-Pro PBD-recognition motif (Supplementary Table S2). An additional four mapped sites contained the motif Ser-pSer, which would also be expected to bind strongly to the PBD (Elia *et al*, 2003b). Among the entire 899 proteins identified in our study, we were able to map an additional 168 phosphorylation sites matching the minimal consensus [pS/pT]P motif for CDKs. Thus, 217/247 or 90% of our mapped sites match the minimal CDK motif, consistent with mitotic arrest.

A large network of proteins involved in cytokinesis is connected by Plk1 PBD ligands

In order to examine one part of the PBD interactome in more detail, we chose to focus on a mitotic process in which Plk1 was thought to be involved, but where many of the details of Plk1-dependent regulation were unclear. At the end of mitosis, the parent cell is cleaved into two daughter cells by a mechanical process known as cytokinesis. During early cytokinesis, the cell elongates and a cleavage furrow is created under the plasma membrane by an actomyosin-based structure known as the contractile ring. The spatial orientation of this ring is controlled by both the central spindle and septins. Later in cytokinesis, the two daughter cells remain connected by a cytoplasmic bridge called the midbody, until abscission, when the two cells separate (Glotzer, 2005). Cells lacking or inappropriately overexpressing certain components for many of these processes fail to complete cytokinesis, resulting in either cells arrested at the midbody stage, or as binucleated cells. In budding and fission yeast, cytokinesis seems to be highly dependent on the fungal homologue of Plk1 (Lee *et al*, 2005). In mammalian cells, there are data implicating Plk1 in the cytokinetic process, but exactly how Plk1 is connected to the network of core cytokinesis components is unknown. In addition to the incompletely understood role of Plk1, regulation of cytokinesis is under the direct control of several other protein kinases including CDK1, AuroraB, and the Rho-regulated protein kinases; Rock1, Rock2, and Citron kinase.

To evaluate additional roles of Plk1 in regulating cytokinesis, we examined protein–protein interactions known to be involved in this process. First, we constructed models of cytokinesis subnetworks for core protein–protein interactions controlling central spindle organization, myosin activation, and actin dynamics based on recent summaries and reviews (Robinson and Spudich, 2004; Glotzer, 2005) with interaction data taken from the Human Protein Reference Database (Mishra *et al*, 2006) (Figure 4B–D). We then constructed a similar model of the subset of Plk1-interacting proteins relevant to cytokinesis by searching for proteins with described cytokinesis phenotypes that were also known to interact with Plk1 from published literature (Figure 4A) (Neef *et al*, 2003; Zhou *et al*, 2003; Daniels *et al*, 2004; Litvak *et al*, 2004; Liu *et al*, 2004; Zhang *et al*, 2004; Fabbro *et al*, 2005; Yamaguchi *et al*, 2005). As seen in Figure 4E, published data allow only one direct link to be constructed between Plk1 and the core cytokinesis processes of actin dynamics and myosin activation, through the Rho-GEF Ect2. Plk1 can bind to and phosphorylate Ect2, and Ect2 depletion results in cytokinesis defects (Niiya *et al*, 2006), but the likely direct connection between Plk1 and cytokinesis through Ect2 has not yet been definitively shown. In budding yeast, however, we recently showed that the yeast Plk1 orthologue Cdc5 directs the localization of the RhoGEFs, Tus1 and Rom2, to the bud neck (the budding yeast equivalent of the mammalian furrow/midbody) and that Cdc5 phosphorylation of Tus1 is necessary for cells to complete cytokinesis (Yoshida *et al*, 2006). The only other published link connecting Plk1 to core components of the cytokinesis network is through the intermediate filament protein vimentin, which appears to be a critical substrate of both Rock and Plk1 (Goto *et al*, 1998; Yamaguchi *et al*, 2005) necessary for completion of cytokinesis.

We next examined which of the core cytokinesis proteins in panels B–D showed mitosis-dependent interactions with the Plk1 PBD in our screen (Figure 4F, yellow circles). This revealed a total of 11 new putative Plk1-modulated core cytokinesis interactions, including potential roles for Plk1 in the direct regulation of several Rho-dependent kinases (Figure 4F, circled red). To identify additional links between Plk1 and these core cytokinetic subnetworks, we expanded the network to include Plk1 PBD-interacting proteins identified in our screen that had previously been experimentally validated to make direct protein–protein interactions with components of these core subnetworks (Figure 4G, green circles). This resulted in creation of a more extended Plk1 PBD-annotated cytokinesis network that contained 27 new

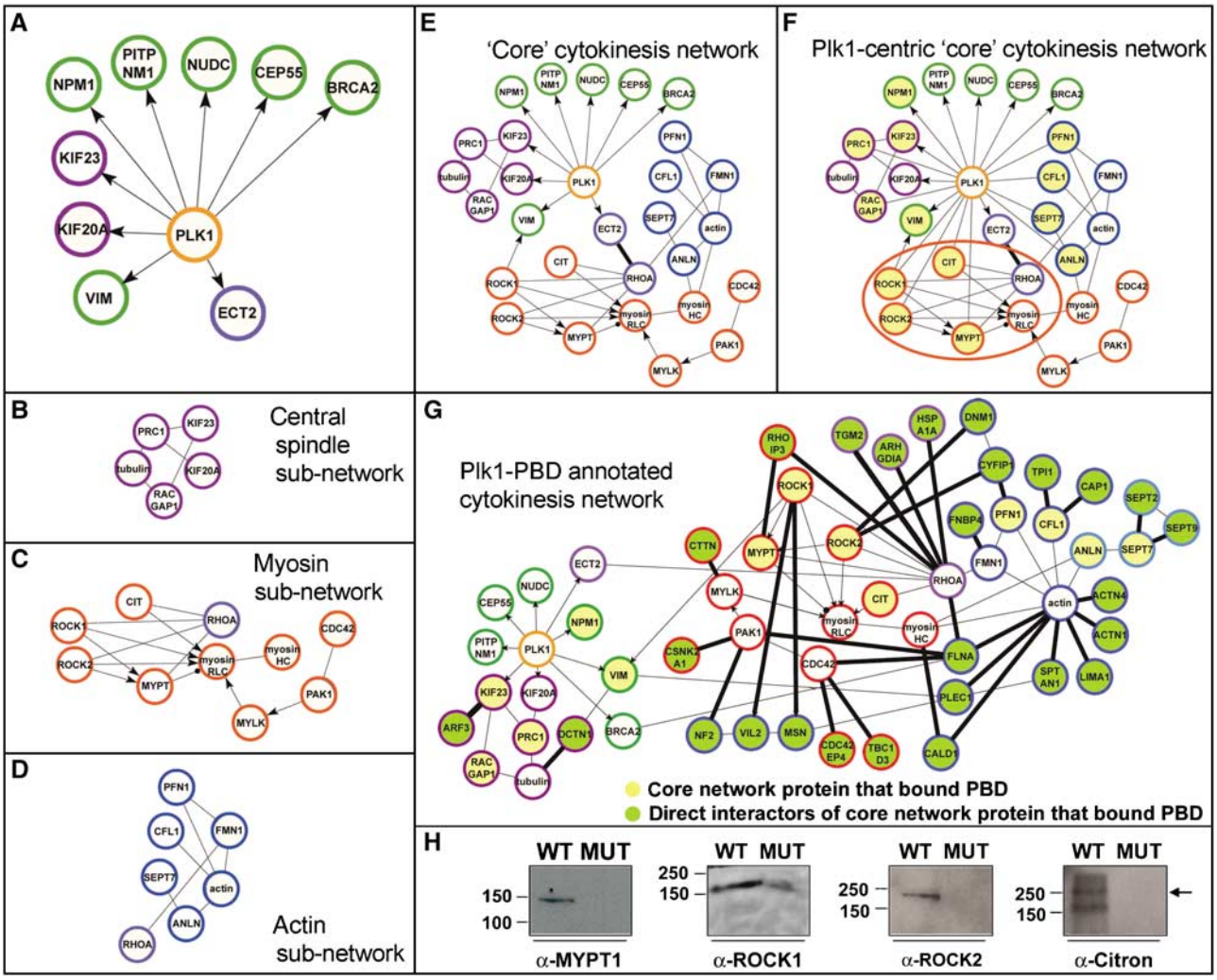

Figure 4 A data-driven Plk1-related cytokinesis network. Circle color coding: orange, Plk1; red, myosin activation network; blue, actin dynamics network; light purple, proteins bridging the actin and myosin networks; dark purple, central spindle organization network; green, proteins not known to function as part of any core cytokinesis network. Proteins are labeled using HUGO gene nomenclature except for actin, tubulin, myosin, and myosin light chains. Myosin phosphatase is shown generically as a node labeled MYPT (official gene symbol for the protein we identified is PPP1R12A). Lines indicate direct protein–protein interactions, arrows indicate a kinase–substrate relationship, and the filled circle between MYPT and myosin RLC indicates a phosphatase–substrate relationship. (**A**) The known Plk1 network of proteins that participate in cytokinesis. (**B**) The core cytokinesis network of central spindle organization. (**C**) The core cytokinesis network of myosin activation. (**D**) The core cytokinesis network of actin dynamics. (**E**) Core cytokinesis network. The networks from (A–D) are shown connected by all of the direct, experimentally verified, protein–protein interactions. The thick line between Ect2 and RhoA represents the only mechanistic connection between previously known Plk1-interacting proteins and the actomyosin cytokinesis subnetworks. (**F**) Plk1-centric core cytokinesis network. The network in panel (E) is redrawn with additional interactions between Plk1 and core network components as revealed by the Plk1 PBD interactome screen. Core cytokinesis network components detected in the Plk1 PBD interaction screen are shaded yellow. Red circle indicates the section of the network selected for further study. (**G**) A Plk1-PBD annotated cytokinesis network. A view of the core cytokinesis network expanded to include additional Plk1 PBD-interacting proteins that were detected in our screen and are known to participate in protein–protein interactions with one or more of the core cytokinesis components. Yellow shading indicates PBD-interacting proteins in the core network; green shading indicates PBD-interacting proteins that also interact with proteins in the core network; thick black lines denote interactions between core network proteins and the additional Plk1 PBD-interacting proteins in the expanded network. (**H**) Proteins within the red circled region from panel (F) were investigated as in Supplementary Figure S1.

PBD-binding proteins that touch the core cytokinesis components to form another 33 potential Plk1-regulated links (Figure 4G, thick black lines, and Supplementary Figure S3).

Plk1 colocalizes with Rock2 during cytokinesis and works synergistically with RhoA to stimulate Rock2 kinase activity

The large set of potential Plk1-regulated cytokinesis proteins revealed by this mass spectrometry/proteomics approach exceeded our capacity to directly investigate in an experimentally tractable manner. We therefore focused our attention on the subset of Rho-regulated protein kinases and phosphatases in the core cytokinesis network that control myosin activation (Figure 4F, circled red). We confirmed that each of these proteins—Rock1, Rock2, Citron kinase, and MYPT1—bound to the Plk1 PBD in a phospho-dependent manner (Figure 4H), and proceeded to investigate Rock2 in more detail.

Rock2 contains an N-terminal kinase domain and a C-terminal Rho-binding domain and PH domain (Figure 5A), and phosphorylates myosin regulatory light chain and myosin phosphatase targeting subunit in a manner that is enhanced upon RhoA binding (Matsumura, 2005). To demonstrate an interaction between full-length Rock2 and Plk1 within cells, myc-tagged Rock2 and Flag-tagged Plk1 containing either a wild-type or mutant PBD were coexpressed in U2OS cells. Lysates were collected from asynchronous and mitotically arrested cells. Immunoprecipitation of the lysates using anti-Flag M2 beads revealed a strong mitosis-dependent interaction of full-length Plk1 containing a wild-type PBD, but not a mutant PBD, with Rock2 (Figure 5B and C). Furthermore, this Plk1–Rock2 interaction was lost when the lysates were treated with λ-phosphatase, confirming that the interaction between the full-length proteins was phospho-dependent (Figure 5D). We also observed significant colocalization of the endogenous proteins during cytokinesis, most prominently at the midbody (Figure 5E), consistent with previously published localization data for each of these proteins individually (Kosako *et al*, 2000; Neef *et al*, 2003).

To investigate whether Rock2 could serve as a substrate for Plk1, full-length bovine Rock2 (Rock2-FL) as well as N-terminal kinase domain- (Rock2-CAT) and C-terminal RBD and PH domain-containing fragments (Rock2-RBD/PH) of Rock2 were phosphorylated by the Plk1 kinase domain *in vitro* in the presence of [γ-^{32}P]ATP (Supplementary Figure S4). Radioactivity was incorporated into all three fragments of Rock2. When *in vitro*-phosphorylated full-length Rock2 was analyzed by mass spectrometry, phosphorylated peptides from only the C-terminal part of the molecule were detected, corresponding to residues Thr-967 (DA*p*TI), Ser-1099 (EE*p*SQ), a monophosphorylated species phosphorylated on one of three consecutive serines from Ser-1132 to Ser-1134 (Figures 5A and Supplementary Figures S4 and S5), and Ser-1374 (NQ*p*SI). Three of these mapped sites conform to the general Plk1 kinase consensus motif [E/D]X[S/T] assuming that the third site is actually Ser-1133 (DS*p*SSI), whereas the fourth site at Ser-1374 contains an N in the −2 position. This pSer-2 Asn has recently been reported in several mapped phosphorylation sites targeted by Cdc5 (Brar *et al*, 2006), and fits with our unpublished data on the *in vitro* Plk1 phosphorylation consensus motif (J Alexander and MB Yaffe, unpublished data). In addition, Ser-1374 phosphorylation was reported in a high-throughput phospho-proteomics screen (Beausoleil *et al*, 2006), indicating that it is phosphorylated *in vivo*. All four of these motifs are conserved in bovine, mouse, rat, and human Rock2. The most likely candidate Plk1 N-terminal site in Rock2 on the basis of consensus motif matching is Thr-489, which is contained in a very acidic stretch of sequence, and peptides containing this site were not recovered in either a phosphorylated or nonphosphorylated form.

To assess the functional significance of Rock2 phosphorylation by Plk1, myc-tagged bovine Rock2 was immunoprecipitated from 293T cells and its kinase activity assayed using a substrate peptide from its physiological substrate, myosin regulatory light chain (Figure 5F). Following phosphorylation, the myosin regulatory light chain peptide substrate was recovered from solution by spotting onto P81 paper and the incorporated radioactivity measured by scintillation counting. The addition of GTP-loaded RhoA increased the basal activity of Rock2 by ~3-fold, similar to the two-fold increase reported previously (Ishizaki *et al*, 1996). Intriguingly, phosphorylation of Rock2 by Plk1 resulted in a similar two-fold elevation of Rock2 kinase activity even in the absence of RhoA-GTP, whereas Plk1 phosphorylation in combination with RhoA resulted in an even more dramatic six-fold enhancement. Control reactions containing RhoA-GTP, Plk1, and myosin regulatory light chain substrate peptide did not result in detectable peptide phosphorylation in the absence of Rock2, nor did additional control reactions containing RhoA-GTP, Plk1 and Rock2 but no peptide substrate. Therefore, the data in Figure 5B–F, taken together, suggest that both Plk1 phosphorylation of Rock2 and RhoA-GTP binding may act synergistically to maximize the kinase activity of Rock2.

To further verify that Plk1 phosphorylation directly activated Rock2, we constructed a mutant version of Rock2 lacking all four Plk1 phosphorylation sites (Rock2-4A). Both wild-type Rock2 and Rock2-4A had similar basal RhoA-activated kinase activity *in vitro* towards myosin regulatory light chain in the absence of Plk1 (Figure 6A, lanes 1 and 2). Following pre-incubation of the wild-type and 4A mutant of Rock2 with Plk1, only the wild-type Rock2, but not the Rock2-4A mutant, showed enhanced protein kinase activity (Figure 6A, lanes 3 and 4).

In order to investigate the potential relevance of Plk1 phosphorylation of Rock2 within cells, it was necessary to devise an assay in which Rock2 activity resulted in a specific cellular phenotype. Because the pathways controlling actomyosin ring contraction during cytokinesis are highly redundant, with at least three kinases other than Rock2 able to phosphorylate myosin regulatory light chain (Matsumura, 2005), simple knockdowns or knockouts of several of these kinases result in very mild or absent phenotypes. For example, elimination of Rock2 alone, or even both Rock2 and Rock1 by siRNA causes only a slight increase in the population of multinucleated cells (Yokoyama *et al*, 2005; data not shown). We therefore took advantage of the fact that completion of cytokinesis requires that the activity of RhoA and Rock2 be shut off in order to allow disassembly of the actomyosin ring (Emoto *et al*, 2005). Overexpression of Rock2 prevented this disassembly and resulted in delay or failure of cells at the midbody stage to complete cytokinesis (Figure 6B).

We used siRNA to deplete endogenous Rock2, while simultaneously overexpressing either the wild-type or 4A mutant forms of Rock2, and examined an asynchronous population of Rock2-overexpressing cells for failure of cytokinesis exit. As seen in Figure 6C, by 24 h after transfection, over one-third of the cells that overexpressed wild-type Rock2 and were in mitosis appeared to be in cytokinesis, compared to ~15% of the control cells. In contrast, overexpression of the Rock2-4A mutant that cannot undergo Plk activation reduced the percentage of mitotic cells that were in cytokinesis by about 50% compared to the wild-type Rock2. By 72 h following transfection, overexpression of wild-type Rock2 resulted in a marked increase in the population of cells with ⩾4N DNA content (Figure 6D and E), consistent with the emergence of binucleated cells capable of undergoing additional rounds of DNA replication, similar to what is seen in cells with persistently active RhoA (Wolf *et al*, 2006). This phenotype was significantly diminished in the cells overexpressing the

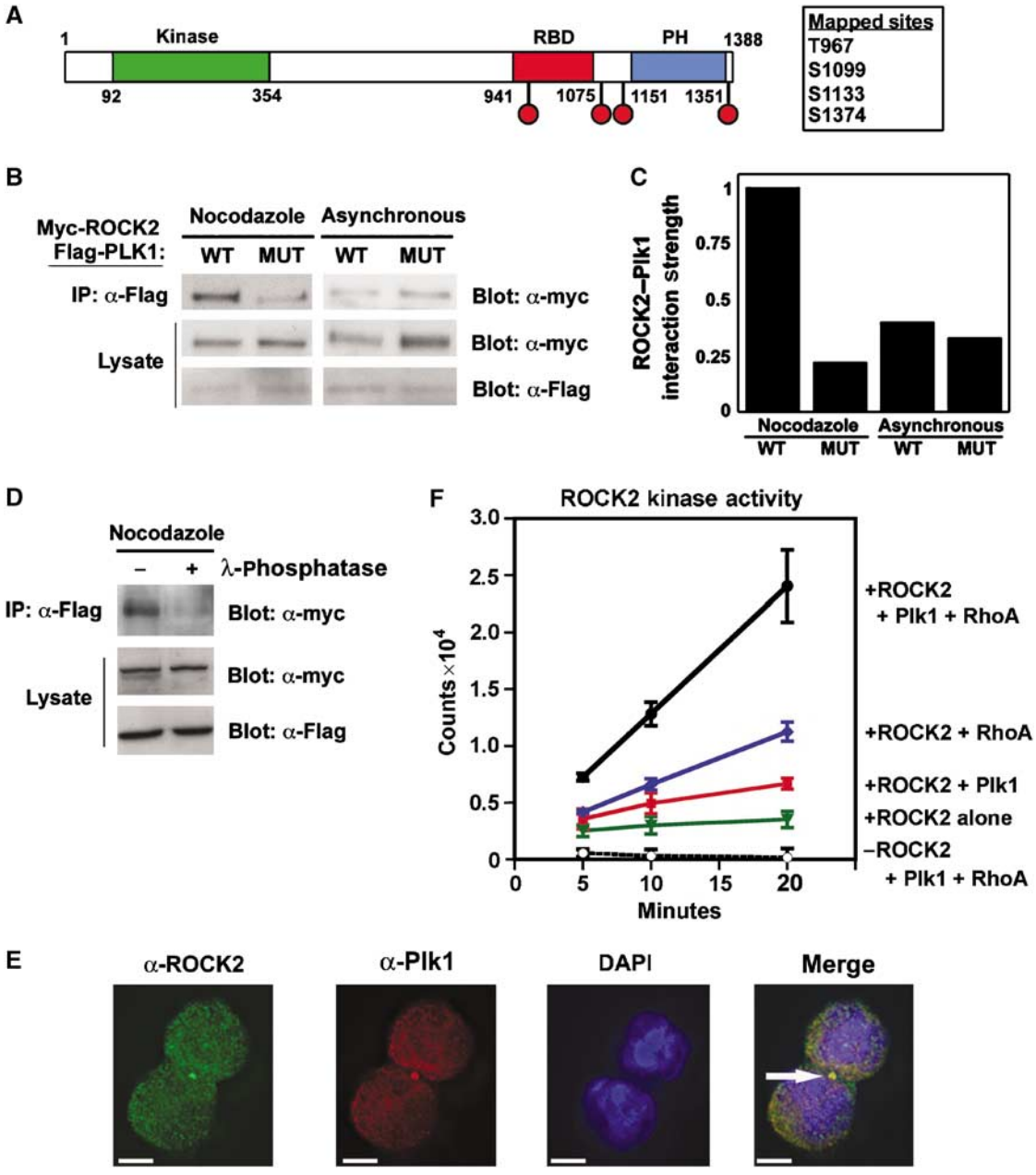

Figure 5 Plk1 and RhoA synergistically activate Rock2. (**A**) Domain structure of Rock2, with amino-acid sequence indicated below. Plk1-dependent phosphorylation sites were mapped by mass spectrometry and are indicated by filled red circles. (**B**) Plk1 and Rock2 interact in cells during mitosis. Full-length myc-tagged Rock2 and Flag-tagged Plk1 (containing wild-type (WT) or mutant (MUT) PBD) were expressed in U2OS cells. Lysates from asynchronous cells or following mitotic arrest with nocodazole were immunoprecipitated using M2 α-Flag beads, and immunoblotted for myc as shown. Note that expression of the MUT Plk1 was much higher than the WT Plk1 as expected, as overexpression of WT Plk1 is somewhat toxic to cells (Mundt *et al*, 1997; Jang *et al*, 2002). (**C**) The amount of Rock2 co-precipitating with Plk1 in (B) was quantified by normalization relative to the level of Rock2 expression. (**D**) Rock2 binding to Plk1 in mitosis is phosphorylation-dependent. Myc-tagged Rock2 and Flag-tagged Plk1 were coexpressed in U2OS cells. Mitotic lysates were prepared from nocodazole-arrested cells, treated for 2 h with λ protein-phosphatase or mock treated, and then immunoprecipitated using M2 α-Flag beads and immunoblotted for myc. (**E**) Rock2 and Plk1 colocalize at the midbody during cytokinesis. U2OS cells were released from a nocodazole block, and fixed and1 h later stained for endogenous Plk1 and Rock2. DNA was stained with DAPI. Deconvolution images are shown. Scale bars = 5 μm. (**F**) Plk1 and RhoA synergize to amplify Rock2 kinase activity. Myc-Rock2 was immunoprecipitated from asynchronous cells and kinase activity against a myosin light chain peptide assayed in the presence or absence of RhoA and/or in response to Rock2 phosphorylation by Plk1. Error bars represent the s.d. of three independent experiments.

Rock2-4A mutant in which Plk1 cannot enhance Rock2 kinase activity. Together, this data suggest that Plk1 can phosphorylate Rock2 *in vivo* to regulate its activity.

In summary, our study has identified over 600 new mitotic phosphorylation-dependent PBD ligands, and suggests an additional function for Plk1 in regulating the kinase activity of at least one of the RhoA effector kinases, Rock2, at specific subcellular mitotic structures, in a manner that synergizes with RhoA-GTP binding as part of a novel mechanism for Rock2 activation (Figure 6F). These findings suggest that Plk1 may participate in two distinct but synergistic processes to maximally activate Rock2, first by facilitating the localized

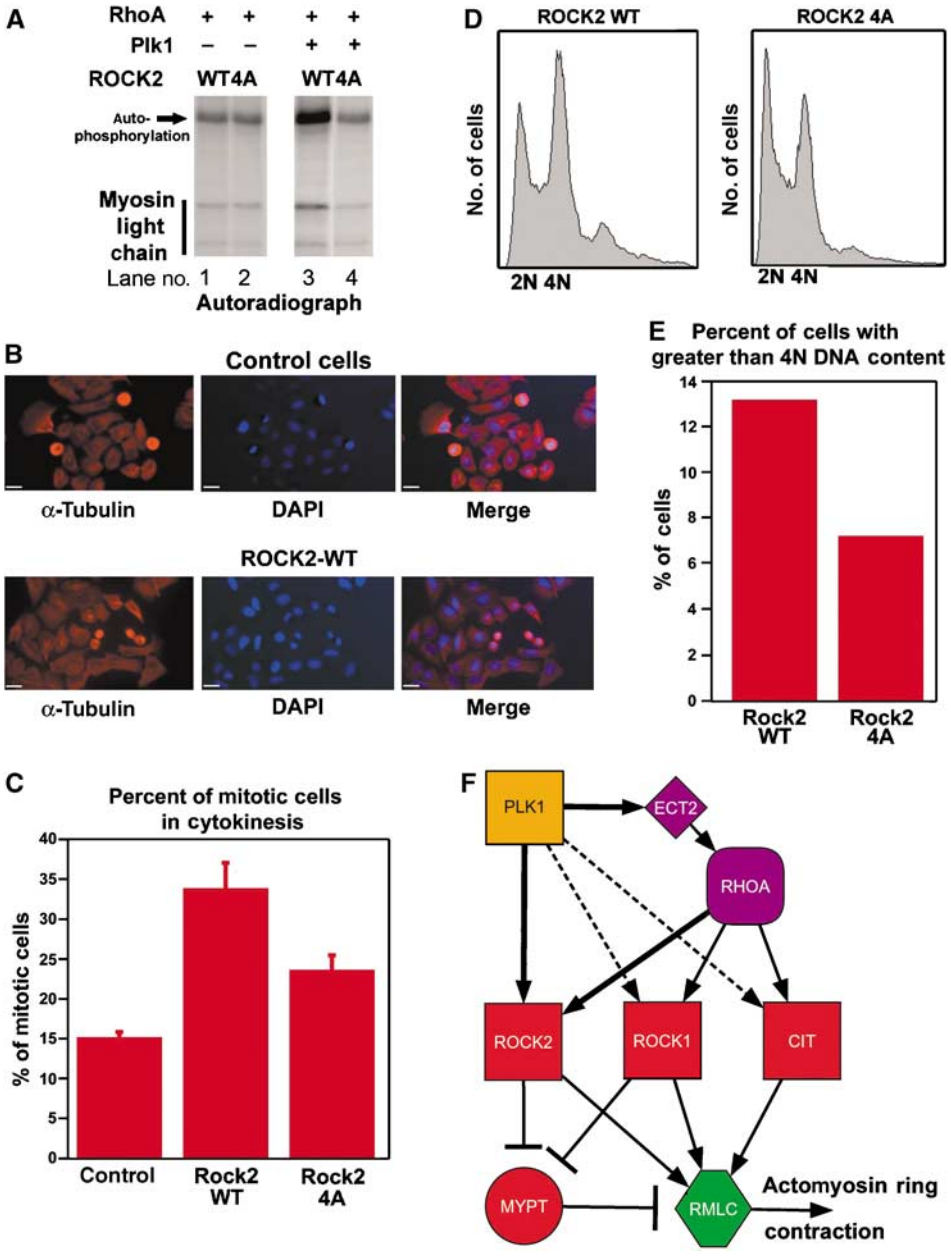

Figure 6 Plk1 activates Rock2 in cells. (**A**) Myc-Rock2 or myc-Rock2-4A was immunoprecipitated from asynchronous cells. Each IP was split in half and one-half has preincubated with Plk1 for 60 min in the presence of cold ATP. Following additional washing, Rock2 kinase activity against myosin regulatory light chain was assayed in the presence of RhoA and [γ-^{32}P]ATP, and analyzed by SDS–PAGE/autoradiography. A strong Rock2 autophosphorylation band is also present. Lanes 1 and 2 in the left panel and lanes 3 and 4 in the right panel are each from the same gel and autoradiograph allowing direct comparison. (**B**) Overexpression of Rock2 causes accumulation of cells in terminal cytokinesis. Asynchronous U2OS cells were transfected with pEF-BOS (control) or pEF-BOS-expressing wild-type Rock2. Mitotic cells from the control transfections displayed a normal rounded-up morphology, whereas many of the mitotic cells overexpressing Rock2 appeared to be in the terminal midbody stage of cytokinesis. Scale bars = 10 μm. (**C**) Percentage of mitotic cells in cytokinesis 24 h after transfection with myc-Rock2, myc-Rock2-4A, or control vectors. Mean values and s.d. from $n = 3$ experiments. (**D**) FACS profiles of cells 72 h after transfection with myc-Rock2 or myc-Rock2-4A. (**E**) Percentage of cells containing greater than 4N DNA content from FACS profiles above. These results are representative of $n = 3$ independent experiments. (**F**) A model of Plk1 control of regulatory myosin light chain (RMLC) phosphorylation during cytokinesis. Arrows indicate activation events and bars indicate inhibition events. Kinases are indicated as squares, phosphatases as circles, GEFs as diamonds, and small G-proteins as rounded squares.

exchange of RhoA-GTP for RhoA-GDP via Ect2 or other GTP-exchange factors, and second, by directly activating the RhoA-GTP effector kinase itself. The experimental analysis of the Plk1 PBD interactome places Plk1 at the center of a large network of mitotic protein–protein interactions, and suggests that Plk1 may play a much larger role than previously appreciated in regulating diverse aspects of mitosis.

Materials and methods

Isolation of PBD-interacting proteins

Wild-type and mutant PBD protein was coupled to CNBr-activated Sepharose 4B beads (Amersham Biosciences) according to the manufacturer's instructions. The beads were transferred to a column and excess PBD washed away with Wash Buffer I (0.1 M Tris (pH 8), 0.5 M NaCl, and 1 mM DTT). The column was

equilibrated with Wash Buffer II (50 mM Tris (pH 8), 0.2 M NaCl, 2 mM DTT, and 10 mM NaF), and the beads then incubated with U2OS cell lysate overnight. Unbound proteins were washed away with 10 column volumes Wash Buffer II. PBD interacting proteins were eluted by incubating the beads with 2 ml of 1 mM phosphopeptide (YMQS-pT-PK) in Wash Buffer II for 1 h at 4°C. The beads were washed with additional 2 ml of the phosphopeptide-containing buffer.

Mass spectrometry

Concentrated eluates from the wild-type and mutant PBD columns were boiled in reducing sample buffer containing β-mercaptoethanol, separated by SDS–PAGE, and visualized by SYPRO Ruby staining (Bio-Rad). Lanes from the gel were excised, cut into 12 fields as shown in Figure 1E and digested overnight at 37°C with an excess of sequencing grade trypsin. Peptides were extracted from the gel with 50% acetonitrile/0.1% formic acid and concentrated in a Speed-Vac. Tryptic digests were analyzed with an automated nano LC/MS/MS system, using a 1100 series autosampler and nano pump (Agilent Technologies, Wilmington, DE) coupled to an LTQ-FT hybrid ion trap Fourier transform mass spectrometer (Thermo Electron, San Jose, CA) equipped with a nanoflow ionization source (James A. Hill Instrument Services, Arlington, MA). Peptides were eluted from a (75 μm × 10 cm) PicoFrit (New Objective, Woburn, MA) column packed with (5 μm × 200 Å) Magic C-18AQ reversed-phase beads (Michrom Bioresources Inc., Auburn, CA) using a 70 min acetonitrile/0.1% formic acid gradient at a flow rate of 250 nl/min to yield ~25 s peak widths. Data-dependent LC/MS/MS spectra were acquired in ~3 s cycles; each cycle was of the following form: one full FT MS scan followed by eight MS/MS scans in the ion trap on the most abundant precursor ions excluding charge 1 and unknown charge, subject to accurate mass, dynamic exclusion for a period of 45 s. Some of the phosphorylation sites were established with additional LC/MS/MS experiments performed on aliquots of the gel band digests with the instrument operated in a targeted mode where MS/MS of 5–17 precursor m/z's were repetitively taken in 3–9 s cycles throughout the acetonitrile gradient. These precursor masses were selected because they correspond to the phosphorylated form of expected tryptic peptides containing S[ST]P motifs derived from proteins confidently identified in aliquots of sample used for the data-dependent experiments. For Rock2 phosphopeptide mapping, both trypsin and chymotrypsin were used to maximize coverage.

Rock2 kinase assays

Myc-tagged Rock2 was preincubated in kinase buffer (50 mM Tris (pH 8), 200 mM NaCl, 2 mM DTT, 5 mM NaF, 200 μM ATP, and 500 μM $MgCl_2$) containing 1 mM GTP with or without 5 μg RhoA and/or 7 ng/μl Plk1 kinase domain for 30 min at 30°C. Reactions were then supplemented with 20 μCi [γ-^{32}P]ATP and 50 μM substrate peptide (Myosin Light Chain Kinase Substrate; AKRPQ-RATSNVFS; Sigma-Aldrich), and aliquots of the reaction spotted onto squares of Whatman P81 paper after an additional 0, 5, 10, or 20 min. The P81 paper was washed with 0.5% phosphoric acid five times, and incorporation of ^{32}P into the substrate peptide was assessed by scintillation counting. For comparison of wild-type and 4A mutant ROCK2, full-length myosin light chain (Sigma) was used as a substrate, and the radiolabeled phosphate incorporation was assessed by autoradiography following SDS–PAGE.

Additional experimental details are provided in Supplementary data.

Supplementary data

Supplementary data are available at *The EMBO Journal* Online (http://www.embojournal.org).

Acknowledgements

We thank K Kaibuchi for providing Rock2 constructs and the MIT CCR Microscopy and Imaging Core Facility. MH is supported by the Danish Medical Research Council. DML was supported by a Howard Hughes Medical Institute Predoctoral Fellowship and is supported by a David Koch Graduate Fellowship. KK is supported by Manpei Suzuki Diabetes Foundation. DL is supported by a Janes Coffin Childs Memorial Fellowship. This work was supported by NIH grant P50-CA112962 to SAC, and GM60594 and a Burrough's Wellcome Career Development Award to MBY.

References

Ahonen LJ, Kallio MJ, Daum JR, Bolton M, Manke IA, Yaffe MB, Stukenberg PT, Gorbsky GJ (2005) Polo-like kinase 1 creates the tension-sensing 3F3/2 phosphoepitope and modulates the association of spindle-checkpoint proteins at kinetochores. *Curr Biol* **15:** 1078–1089

Barr FA, Sillje HH, Nigg EA (2004) Polo-like kinases and the orchestration of cell division. *Nat Rev Mol Cell Biol* **5:** 429–440

Beausoleil SA, Villen J, Gerber SA, Rush J, Gygi SP (2006) A probability-based approach for high-throughput protein phosphorylation analysis and site localization. *Nat Biotechnol* **24:** 1285–1292

Brar GA, Kiburz BM, Zhang Y, Kim JE, White F, Amon A (2006) Rec8 phosphorylation and recombination promote the step-wise loss of cohesins in meiosis. *Nature* **441:** 532–536

Carmena M, Riparbelli MG, Minestrini G, Tavares AM, Adams R, Callaini G, Glover DM (1998) *Drosophila* polo kinase is required for cytokinesis. *J Cell Biol* **143:** 659–671

Cheng KY, Lowe ED, Sinclair J, Nigg EA, Johnson LN (2003) The crystal structure of the human polo-like kinase-1 polo box domain and its phospho-peptide complex. *EMBO J* **22:** 5757–5768

Daniels MJ, Wang Y, Lee M, Venkitaraman AR (2004) Abnormal cytokinesis in cells deficient in the breast cancer susceptibility protein BRCA2. *Science* **306:** 876–879

Darieva Z, Bulmer R, Pic-Taylor A, Doris KS, Geymonat M, Sedgwick SG, Morgan BA, Sharrocks AD (2006) Polo kinase controls cell-cycle-dependent transcription by targeting a coactivator protein. *Nature* **444:** 494–498

De Luca M, Lavia P, Guarguaglini G (2006) A functional interplay between Aurora-A, Plk1 and TPX2 at spindle poles: Plk1 controls centrosomal localization of Aurora-A and TPX2 spindle association. *Cell Cycle* **5:** 296–303

Donaldson MM, Tavares AA, Ohkura H, Deak P, Glover DM (2001) Metaphase arrest with centromere separation in polo mutants of *Drosophila*. *J Cell Biol* **153:** 663–676

Elia AE, Cantley LC, Yaffe MB (2003a) Proteomic screen finds pSer/pThr-binding domain localizing Plk1 to mitotic substrates. *Science* **299:** 1228–1231

Elia AE, Rellos P, Haire LF, Chao JW, Ivins FJ, Hoepker K, Mohammad D, Cantley LC, Smerdon SJ, Yaffe MB (2003b) The molecular basis for phosphodependent substrate targeting and regulation of plks by the polo-box domain. *Cell* **115:** 83–95

Emoto K, Inadome H, Kanaho Y, Narumiya S, Umeda M (2005) Local change in phospholipid composition at the cleavage furrow is essential for completion of cytokinesis. *J Biol Chem* **280:** 37901–37907

Fabbro M, Zhou BB, Takahashi M, Sarcevic B, Lal P, Graham ME, Gabrielli BG, Robinson PJ, Nigg EA, Ono Y, Khanna KK (2005) Cdk1/Erk2- and Plk1-dependent phosphorylation of a centrosome protein, Cep55, is required for its recruitment to midbody and cytokinesis. *Dev Cell* **9:** 477–488

Feng Y, Hodge DR, Palmieri G, Chase DL, Longo DL, Ferris DK (1999) Association of polo-like kinase with alpha-, beta- and gamma-tubulins in a stable complex. *Biochem J* **339** (Part 2)**:** 435–442

Feng Y, Longo DL, Ferris DK (2001) Polo-like kinase interacts with proteasomes and regulates their activity. *Cell Growth Differ* **12:** 29–37

Glotzer M (2005) The molecular requirements for cytokinesis. *Science* **307:** 1735–1739

Glover DM (2005) Polo kinase and progression through M phase in *Drosophila*: a perspective from the spindle poles. *Oncogene* **24:** 230–237

Golsteyn RM, Schultz SJ, Bartek J, Ziemiecki A, Ried T, Nigg EA (1994) Cell cycle analysis and chromosomal localization of human Plk1, a putative homologue of the mitotic kinases *Drosophila* polo and *Saccharomyces cerevisiae* Cdc5. *J Cell Sci* **107** (Part 6)**:** 1509–1517

GO Consortium (2001) Creating the gene ontology resource: design and implementation. *Genome Res* **11:** 1425–1433

Goto H, Kiyono T, Tomono Y, Kawajiri A, Urano T, Furukawa K, Nigg EA, Inagaki M (2006) Complex formation of Plk1 and INCENP required for metaphase–anaphase transition. *Nat Cell Biol* **8:** 180–187

Goto H, Kosako H, Tanabe K, Yanagida M, Sakurai M, Amano M, Kaibuchi K, Inagaki M (1998) Phosphorylation of vimentin by Rho-associated kinase at a unique amino-terminal site that is specifically phosphorylated during cytokinesis. *J Biol Chem* **273:** 11728–11736

Ishizaki T, Maekawa M, Fujisawa K, Okawa K, Iwamatsu A, Fujita A, Watanabe N, Saito Y, Kakizuka A, Morii N, Narumiya S (1996) The small GTP-binding protein Rho binds to and activates a 160 kDa Ser/Thr protein kinase homologous to myotonic dystrophy kinase. *EMBO J* **15:** 1885–1893

Jang YJ, Ma S, Terada Y, Erikson RL (2002) Phosphorylation of threonine 210 and the role of serine 137 in the regulation of mammalian polo-like kinase. *J Biol Chem* **277:** 44115–44120

Kim JH, Paek KY, Choi K, Kim TD, Hahm B, Kim KT, Jang SK (2003) Heterogeneous nuclear ribonucleoprotein C modulates translation of c-myc mRNA in a cell cycle phase-dependent manner. *Mol Cell Biol* **23:** 708–720

Kim SA, Yoon JH, Lee SH, Ahn SG (2005) Polo-like kinase 1 phosphorylates heat shock transcription factor 1 and mediates its nuclear translocation during heat stress. *J Biol Chem* **280:** 12653–12657

Kosako H, Yoshida T, Matsumura F, Ishizaki T, Narumiya S, Inagaki M (2000) Rho-kinase/ROCK is involved in cytokinesis through the phosphorylation of myosin light chain and not ezrin/radixin/moesin proteins at the cleavage furrow. *Oncogene* **19:** 6059–6064

Lane HA, Nigg EA (1996) Antibody microinjection reveals an essential role for human polo-like kinase 1 (Plk1) in the functional maturation of mitotic centrosomes. *J Cell Biol* **135:** 1701–1713

Lee KS, Park JE, Asano S, Park CJ (2005) Yeast polo-like kinases: functionally conserved multitask mitotic regulators. *Oncogene* **24:** 217–229

Litvak V, Argov R, Dahan N, Ramachandran S, Amarilio R, Shainskaya A, Lev S (2004) Mitotic phosphorylation of the peripheral Golgi protein Nir2 by Cdk1 provides a docking mechanism for Plk1 and affects cytokinesis completion. *Mol Cell* **14:** 319–330

Liu X, Lei M, Erikson RL (2006) Normal cells, but not cancer cells, survive severe Plk1 depletion. *Mol Cell Biol* **26:** 2093–2108

Liu X, Lin CY, Lei M, Yan S, Zhou T, Erikson RL (2005) CCT chaperonin complex is required for the biogenesis of functional Plk1. *Mol Cell Biol* **25:** 4993–5010

Liu X, Zhou T, Kuriyama R, Erikson RL (2004) Molecular interactions of Polo-like-kinase 1 with the mitotic kinesin-like protein CHO1/MKLP-1. *J Cell Sci* **117:** 3233–3246

Lowery DM, Lim D, Yaffe MB (2005) Structure and function of Polo-like kinases. *Oncogene* **24:** 248–259

Matsumura F (2005) Regulation of myosin II during cytokinesis in higher eukaryotes. *Trends Cell Biol* **15:** 371–377

Mishra GR, Suresh M, Kumaran K, Kannabiran N, Suresh S, Bala P, Shivakumar K, Anuradha N, Reddy R, Raghavan TM, Menon S, Hanumanthu G, Gupta M, Upendran S, Gupta S, Mahesh M, Jacob B, Mathew P, Chatterjee P, Arun KS, Sharma S, Chandrika KN, Deshpande N, Palvankar K, Raghavnath R, Krishnakanth R, Karathia H, Rekha B, Nayak R, Vishnupriya G, Kumar HG, Nagini M, Kumar GS, Jose R, Deepthi P, Mohan SS, Gandhi TK, Harsha HC, Deshpande KS, Sarker M, Prasad TS, Pandey A (2006) Human protein reference database—2006 update. *Nucleic Acids Res* **34:** D411–D414

Mundt KE, Golsteyn RM, Lane HA, Nigg EA (1997) On the regulation and function of human polo-like kinase 1 (PLK1): effects of overexpression on cell cycle progression. *Biochem Biophys Res Commun* **239:** 377–385

Nakajima H, Toyoshima-Morimoto F, Taniguchi E, Nishida E (2003) Identification of a consensus motif for Plk (Polo-like kinase) phosphorylation reveals Myt1 as a Plk1 substrate. *J Biol Chem* **278:** 25277–25280

Neef R, Preisinger C, Sutcliffe J, Kopajtich R, Nigg EA, Mayer TU, Barr FA (2003) Phosphorylation of mitotic kinesin-like protein 2 by polo-like kinase 1 is required for cytokinesis. *J Cell Biol* **162:** 863–876

Niiya F, Tatsumoto T, Lee KS, Miki T (2006) Phosphorylation of the cytokinesis regulator ECT2 at G2/M phase stimulates association of the mitotic kinase Plk1 and accumulation of GTP-bound RhoA. *Oncogene* **25:** 827–837

Ohkura H, Hagan IM, Glover DM (1995) The conserved Schizosaccharomyces pombe kinase plo1, required to form a bipolar spindle, the actin ring, and septum, can drive septum formation in G1 and G2 cells. *Genes Dev* **9:** 1059–1073

Qian YW, Erikson E, Taieb FE, Maller JL (2001) The polo-like kinase Plx1 is required for activation of the phosphatase Cdc25C and cyclin B-Cdc2 in *Xenopus* oocytes. *Mol Biol Cell* **12:** 1791–1799

Rapley J, Baxter JE, Blot J, Wattam SL, Casenghi M, Meraldi P, Nigg EA, Fry AM (2005) Coordinate regulation of the mother centriole component nlp by nek2 and plk1 protein kinases. *Mol Cell Biol* **25:** 1309–1324

Robinson DN, Spudich JA (2004) Mechanics and regulation of cytokinesis. *Curr Opin Cell Biol* **16:** 182–188

Shin C, Manley JL (2002) The SR protein SRp38 represses splicing in M phase cells. *Cell* **111:** 407–417

Song S, Lee KS (2001) A novel function of *Saccharomyces cerevisiae* CDC5 in cytokinesis. *J Cell Biol* **152:** 451–469

Spankuch-Schmitt B, Wolf G, Solbach C, Loibl S, Knecht R, Stegmuller M, von Minckwitz G, Kaufmann M, Strebhardt K (2002) Downregulation of human polo-like kinase activity by antisense oligonucleotides induces growth inhibition in cancer cells. *Oncogene* **21:** 3162–3171

Straight AF, Field CM, Mitchison TJ (2005) Anillin binds nonmuscle myosin II and regulates the contractile ring. *Mol Biol Cell* **16:** 193–201

Tarnowka MA, Baglioni C (1979) Regulation of protein synthesis in mitotic HeLa cells. *J Cell Physiol* **99:** 359–367

Tsvetkov L, Stern DF (2005) Interaction of chromatin-associated Plk1 and Mcm7. *J Biol Chem* **280:** 11943–11947

van de Weerdt BC, Medema RH (2006) Polo-like kinases: a team in control of the division. *Cell Cycle* **5:** 853–864

van Vugt MA, Bras A, Medema RH (2004a) Polo-like kinase-1 controls recovery from a G2 DNA damage-induced arrest in mammalian cells. *Mol Cell* **15:** 799–811

van Vugt MA, van de Weerdt BC, Vader G, Janssen H, Calafat J, Klompmaker R, Wolthuis RM, Medema RH (2004b) Polo-like kinase-1 is required for bipolar spindle formation but is dispensable for anaphase promoting complex/Cdc20 activation and initiation of cytokinesis. *J Biol Chem* **279:** 36841–36854

Warren G (1993) Membrane partitioning during cell division. *Annu Rev Biochem* **62:** 323–348

Wolf A, Keil R, Gotzl O, Mun A, Schwarze K, Lederer M, Huttelmaier S, Hatzfeld M (2006) The armadillo protein p0071 regulates Rho signalling during cytokinesis. *Nat Cell Biol* **8:** 1432–1440

Yamaguchi T, Goto H, Yokoyama T, Sillje H, Hanisch A, Uldschmid A, Takai Y, Oguri T, Nigg EA, Inagaki M (2005) Phosphorylation by Cdk1 induces Plk1-mediated vimentin phosphorylation during mitosis. *J Cell Biol* **171:** 431–436

Yokoyama T, Goto H, Izawa I, Mizutani H, Inagaki M (2005) Aurora-B and Rho-kinase/ROCK, the two cleavage furrow kinases, independently regulate the progression of cytokinesis: possible existence of a novel cleavage furrow kinase phosphorylates ezrin/radixin/moesin (ERM). *Genes Cells* **10:** 127–137

Yoshida S, Kono K, Lowery DM, Bartolini S, Yaffe MB, Ohya Y, Pellman D (2006) Polo-like kinase Cdc5 controls the local activation of Rho1 to promote cytokinesis. *Science* **313:** 108–111

Zhang H, Shi X, Paddon H, Hampong M, Dai W, Pelech S (2004) B23/Nucleophosmin serine 4 phosphorylation mediates mitotic functions of Polo-like kinase 1. *J Biol Chem* **279:** 35726–35734

Zhou T, Aumais JP, Liu X, Yu-Lee LY, Erikson RL (2003) A role for Plk1 phosphorylation of NudC in cytokinesis. *Dev Cell* **5:** 127–138